Research on Temporal Patterns of Water−Rock Interaction in the Coal Mine Underground Reservoir Based on the Dynamic Simulation Test

Shuyu Liu, Kai Zhang,* Ju Gao, Yingming Yang, Lu Bai, and Jiayu Yan

Read Online

ACCESS | Metrics & More | Article Recommendations

ABSTRACT: The temporal pattern of water−rock interaction is significant in predicting the ion concentration of the effluent in coal mine underground reservoirs. This study used the roof-caved rock samples and main incoming water (mine water and fissure water) of the Daliuta coal underground reservoir as the research object and designed four groups of dynamic simulation experiments of the water−rock interaction. Based on the main ion concentrations in the water sample at different reaction times, Q-type hierarchical cluster analysis (HCA) was used to classify the stages of water−rock interaction. The types and intensities of water−rock interaction in each stage were identified by combining the ion ratio and principal component analysis (PCA). Q-type HCA shows that the dynamic simulation experimental water samples can be divided into three categories according to the reaction time, representing the early, middle, and late stages of the water−rock interaction process. The influence of water quality on the division of the water−rock interaction stage is greater than that of rock characteristics. The ion ratio and PCA show that the dissolution of pyrite minerals, cation exchange reaction, and mineral adsorption mainly occur in the early stage of water−rock interaction, in which the cation exchange reaction plays a leading role in the change of ions in water. In the middle stage, the cation exchange reaction and the dissolution of carbonate minerals, such as calcite and dolomite, mainly occur, in which mineral dissolution is the main. In the late stage, the water−rock interaction is relatively weak, and the change of ion concentration in water is not obvious. This study proves the temporal patterns of water−rock interaction between caved rock and mine water (or fissure water) and differences in the types and intensities of water−rock interaction in each stage. The results can provide a theoretical basis for the optimization of the operation cycle of coal mine underground reservoirs and the prediction of effluent ion concentration.
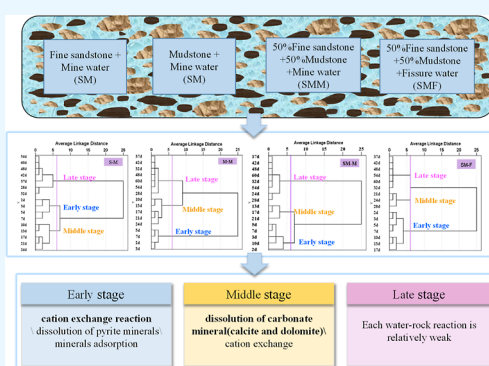
1. INTRODUCTION

The western region (Shanxi, Shaanxi, Mongolia, and Gansu) has the largest coal production potential in China, accounting for 70% of the country's annual coal output but only about 4% of the country's water resource distribution.[1−3] At the same time, the region also has ecological and environmental problems, such as desertification and severe soil erosion.[4,5] The serious shortage of water resources and the fragile ecological environment restrict the development and utilization of coal resources in this region.[6,7] Given the above problems, Gu proposed and developed the coal mine underground reservoir technology, which is used to transfer, purify, store, and utilize of mine water using the cavity of broken rock mass in the goaf after coal mining.[8−10] This technology realizes the efficient recycling of water resources and does not destroy the surface eco-environment, which is significant to the sustainable development of mining areas in Western China.[11,12]

With the application of underground reservoir technology, some scholars found that the water quality of mine water was significantly improved after being stored in the underground reservoir, and the concentration of pollutants such as suspended solids, chemical oxygen demand (COD), heavy metal ions, and TDS was significantly reduced.[13−15] For example, the field investigation found that the suspended solids, turbidity, and COD in the effluent of the Daliuta underground reservoir decreased significantly; TDS decreased by 162 mg/L; the concentration of Na^+ and Cl^- increased, while the concentration of Ca^{2+} decreased; the hydrochemical type changes from $Cl + SO_4−Ca + Na$ of inlet water to $Cl + SO_4−Na + Ca$ of outlet water;[16,17] based on the indoor simulation experiment, some scholars analyzed the water−rock interaction process from the

changes in ion concentration and rock properties. They deduced that the process mainly occurred through the dissolution of minerals (i.e., dolomite and albite), adsorption, and cationic exchange.[18,19] Although the types of water−rock interaction have been clarified, current research focuses on the entire process of water−rock interaction, ignoring the effect of occurrence time on the type and intensity of water−rock interaction. In fact, due to the dynamic change of the storage capacity of the underground reservoir, the mine water will stay for some time after entering the reservoir, and the residence time ranges from more than ten days to several hundred days. The residence time has a significant impact on the concentration of main ions in the outflow water, which is due to the mixing effect caused by the constant replenishment of water in the reservoir and the coupling effect of various water−rock reactions.[20,21] Generally speaking, with the extension of residence time, the treatment effect of various pollutants (suspended solids, heavy metals, TDS, COD, etc.) is better. The water from the underground reservoir of the coal mine is mainly used for two purposes, one for surface water reuse and the other for underground water recycling. The concentration level of main ions in water determines the type of surface water utilization (industrial water, landscape water, domestic water, etc.).[9,22,23] Therefore, it is of practical significance to know the change in the effluent ion concentration of the underground reservoir with the residence time for predicting the effluent ion concentration and guiding the subsequent utilization of water resources.

The change of ions in the effluent water of the underground reservoir is mainly affected by the water−rock interaction between the incoming water in the underground reservoir and the overlying collapsed rocks. Given the great uncertainty caused by natural factors (caved rock characteristics, overlying fissure water quality, and geological structure) and human interference (mine water quality and residence time), the characterization of water−rock interaction in coal mine underground reservoirs is challenging.[24,25] The chemical elements in groundwater largely depend on the dissolution/precipitation mode of minerals in the aquifer matrix.[26] The ion ratio method, correlation analysis, and principal component analysis (PCA) are effective methods to identify the causes of ions in groundwater.[27] In addition to these traditional methods, many researchers have integrated multivariate statistical and geochemical modeling to interpret complex hydro-chemical datasets, allowing detailed characterization of groundwater chemical evolution.[28−30] Hierarchical cluster analysis (HCA) is an effective technique of multivariate statistics, which can be divided into R-type HCA and Q-type HCA.[31,32] The role of R-type HCA is similar to PCA, which can cluster the variables reflecting the characteristics of samples to classify the indicators into a few data sets. In contrast, the role of Q-type HCA is to classify water samples with complex chemical data sets to reduce the duality of multivariable chemical data sets.[33,34]

The ion concentration of water out of the underground water reservoir in the coal mine is closely related to the operation time, and there may be a temporal pattern of water−rock interaction processes affecting the ion concentration changes. In order to prove this hypothesis, this study selected the roof-caved rock and main incoming water (mine water and fissure water) of the Daliuta coal mine underground reservoir as the research object. The dynamic simulation experiment of the water−rock interaction comparing the water quality and rock properties was designed based on the analysis of the original water sample and rock sample characteristics. The main research purposes are

as follows: (1) according to the main ion concentrations of water samples at different reaction times in the simulation experiment, the temporal patterns of water−rock interaction were defined by Q-type HCA; (2) the main ion sources of each stage are analyzed by the ion ratio method; (3) combined with PCA method, the type and intensity of water−rock interaction at each stage are revealed. This study is of practical significance to water quality control and optimization of the operation cycle of the coal mine underground reservoirs.

2. MATERIALS AND METHODS

2.1. Study Area. This study chose a coal mine underground reservoir located in the Daliuta coal mine (39°13′53″N-39°21′32″N and 110°12′23″E-110°22′54″E) of the Shendong mining area, the largest coal base in China. Shendong mining area is dry and rainless. The average annual precipitation in most areas is only 100−400 mm, and the per capita water resource is only 200−400 m,[3] which is a serious water shortage area. At the same time, many large-scale energy and chemical bases have been established in the mining area, and a large amount of water resources are required for normal operation and daily life. In addition, a large amount of mine water formed by coal mining has high salt and sulfur, which has a certain negative impact on the quality of groundwater resources, the use of underground equipment, and the recycling of surface water resources.[11] The goal of the underground reservoir is to use the voids in the caving zone, diversion fracture zone, and curved settlement zone to store water to adjust the temporal and spatial distribution of water resources,[35] as shown in Figure 1. The objects of
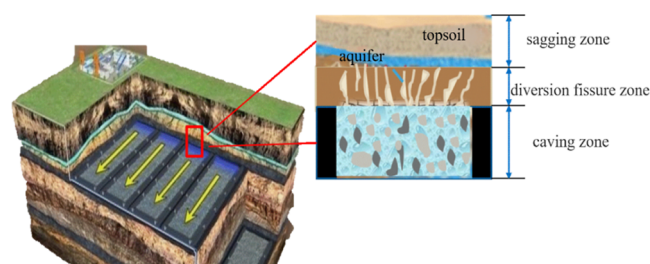

Figure 1. Distributed underground reservoir in Daliuta coal mine.[13] Adapted or reprinted in part with permission from [Chen, S. Research on the Key Technology of Water Resources Recycling Utilization in the Underground Goaf Reservoir in Shendong Mining Area, Xi'an University of Science and Technology, 2016]. Copyright [2016] [Xi'an University of Science and Technology/Chen, S.].

regulation and storage are surface water, groundwater, and underground production wastewater. The mode is to exploit and use the water resource in the wet season and use manual intervention to regulate and store water resources in the dry season. The main components of coal mine underground reservoir technology are water storage engineering, water conservation engineering, surface water seepage prevention engineering, mining engineering, drainage engineering, water treatment engineering, and water quality monitoring and management.[36] The underground reservoirs of nos. 1, 2, and 3 in the Daliuta coal mine have been built using three goafs in the 2^{-2} coal seam, the middle four, the old six, and the new six, with a depth of approximately 130 m. Two water recycling chambers have been built in the gob of the 2^{-2} coal seam. no. 4 underground reservoir is under construction.

2.2. Sample Collection and Pretreatment. Based on the site conditions of the Daliuta coal mine, the location of rock

samples was collected from the roof caving rock of 5^{-2} coal seam. After being sealed and stored, they were transported back to the laboratory for a simulation experiment. Given the limited conditions, five water samples were collected on-site. The inlet and outlet water samples of the reservoir were collected from the reinjection facilities of no. 2 reservoir recharge facilities (S3) and no. 1 reservoir 400 outlets (S4) and 406 outlets (S2) to analyze the impact of the underground reservoir on the quality of mine water. The mine water samples (S1) and fissure water samples (S5) used in the simulation experiment were collected in the water recycling chamber and the side waterway of the coal mining face in the 5^{-2} coal seam, respectively.

According to the apparent morphology, the collected rock samples can be divided into two types. One is fine sandstone with fine and dense sand on the surface, and the other is mudstone with a parallel bedding structure,[19] as shown in Figure 2. The two kinds of rocks were crushed to approximately 8 mm
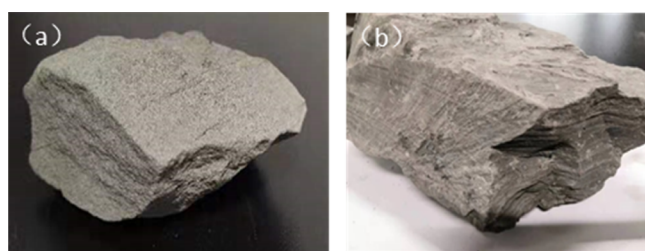

Figure 2. Classification of the macro-appearance of caved rock: (a) fine sandstone and (b) mudstone. Photograph courtesy of "Shuyu Liu". Copyright 2023.

and cleaned with deionized water to remove the surface charge and magazine dust generated in the process of crushing. Then, they were dried in a thermostatic drying oven and cooled at room temperature for later use. The mine water sample and fissure water sample were filtered to remove the SS to prevent the pipeline of the experiment device from blocking, thus interfering with the sample inlet and outlet processes. Then, the filtered water sample was sealed and stored separately for standby.

2.3. Dynamic Simulation Experiment of Water−Rock Interaction.

The device for the dynamic simulation experiment of water−rock interaction is shown in Figure 3. The device comprises a water storage and inlet container, a water−rock interaction reaction column, and a water sample collection container. The column has a height of 30 cm and an inner diameter of 8 cm. A sieve plate was installed at the bottom of the column to support the rock layer. Considering that the change of ion concentration in the outlet water of the underground reservoir is mainly affected by water quality and rock properties, four experimental groups were set up to discuss the impact of water quality and rock properties on water−rock interaction, namely, the water comparison group (50% fine sandstone + 50% mudstone)−mine water (SMM) and (50% fine sandstone + 50% mudstone)−fissure water (SMF), and the rock comparison group is fine sandstone−mine water (SM) and mudstone−mine water (MM). The pretreated rock samples, with a mass of approximately 1.9 kg, were filled into the column, and then, the water samples entered the test column from the water storage and inlet container. The volume density in each test column is 1.27 g/mL, and the effective porosity is 0.428 L/L.

During the experiment, phased methods of injection and sampling were adopted; that is, 200 mL of water sample was injected and sampled into the device at the same time every day (the sampling process lasts for 10 min). The cation and anion concentrations of the water samples were tested on the 2nd, 3rd, 5th, 7th, 10th, 13th, 17th, 21st, 24th, 28th, 32nd, 37th, 42nd, 48th, 54th, and 60th days after the start of the experiment.

2.4. Test Method of Sample Analysis.

The rock samples (fine sandstone and mudstone) were ground to a particle size that could pass through a 200-mesh sieve. A Shimadzu (XRF-800) Japanese Neo-Confucianism (ZSX Primus II) X-ray fluorescence spectrometer was used for qualitative and semi-quantitative analysis of elements. A SmartLab SE type X-ray diffractometer (XRD) (Cu target, Kα radiation, step size of 0.02°, power of 40 kV, 150 mA, continuous scanning) produced by Rigaku Corporation of Japan for mineral composition analysis was used. Test conditions had a 2θ angle range of 5−80° and a scanning speed of 4°/min. The surface morphology of the samples was observed by scanning electron microscopy (Phenom Desktop SEM), produced by Phenom-World
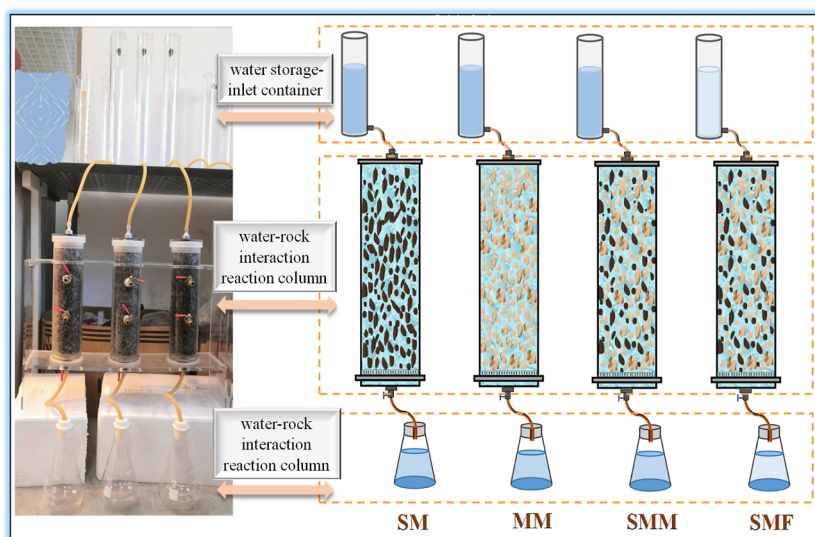

Figure 3. Diagrammatic diagram of the dynamic simulation test. Photograph courtesy of "Shuyu Liu". Copyright 2023.

Table 1. Chemical Composition of Rock Samples for Experiment (%)

composition	SiO_2	Al_2O_3	CO_2	Fe_2O_3	K_2O	Na_2O	MgO	CaO	P_2O_5	SO_3
sandstone	59.199	22.405	6.184	4.168	3.935	1.097	0.864	0.871	0.184	0.076
mudstone	59.641	21.630	8.786	0.384	3.535	1.037	1.324	0.438	0.216	0.060
composition	Cl	TiO_2	ZnO	Cr_2O_3	MnO	Co_2O_3	NiO	CuO	other	
sandstone	0.019	0.835	0.014	0.011	0.039	0.003	0.006	0.003	0.087	
mudstone	0.014	0.895	0.003	0.014	0.038	0.002	0.007	0.005	1.971	
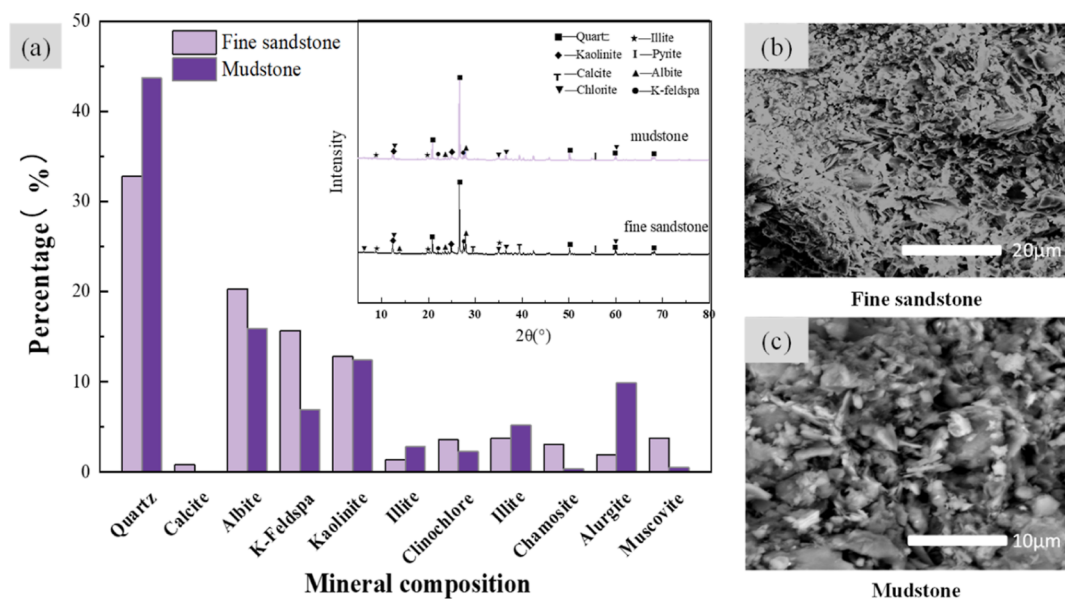
Figure 4. Mineral composition and micromorphology of rock samples: (a) XRD analysis of fine sandstone and mudstone; (b) SEM image of fine sandstone (4000 times); (c) SEM image of mudstone (7700 times).

companies in the Netherlands. The ASAP 2020M Rapid Specific Surface/Pore Analyzer (BET) was used to analyze the specific surface area, total pore volume, and average pore size of the samples.

Referring to the "groundwater quality inspection method" (DZ/T 0064-1993), the physical indexes, such as the visible matter of water samples, were observed and recorded in the field. The pH value and electrical conductivity (EC) of water samples were measured immediately using handheld analyzing kits after the field collection. COD was determined by rapid digestion spectrophotometry. The determination of CO_3^{2-} and HCO_3^- concentrations can be done by double-mixed indicator titration. The concentration of K^+, Na^+, Ca^{2+}, and heavy metals was determined by PerkinElmer NexlON 300D inductively coupled plasma mass spectrometry (ICP-MS) (United States). Each water quality index was repeatedly tested more than three times, and the average value was calculated for subsequent analysis.

2.5. Statistical Analysis Method. First, based on the ion concentration in the dynamic simulation experiment water sample, the Q-HCA method is used to classify the water samples with different reaction times and determine the temporal patterns of water−rock interaction. Second, the ion ratio was calculated to identify the source of the main ion. Meanwhile, combined with one-way variance, the effects of different water−rock interaction conditions and action stages on the ion source were analyzed. Finally, the main ions were classified by PCA to comprehensively judge the reaction types and degrees in different stages of the water−rock interaction.

3. RESULTS

3.1. Characteristic Analysis of Rock Samples. The source and concentration change of ions in mine water are closely related to the properties of underground reservoir rock samples. The differences between the two types of rocks are understood from the aspects of chemical composition, mineral composition, surface morphology, and structure of rocks, which provides a certain basis for revealing the mechanism of the water−rock interaction. Using the XRF, the spectral semi-quantitative mineral element composition analysis results of rock samples were detailed in Table 1. The main elements of rock samples were Si and Al, and the total proportion of corresponding oxides SiO_2 and Al_2O_3 was 81.6 and 81.3%, respectively. These elements were followed by a small amount of C, Fe, K, Na, Mg, Ca, S, and Cl. The types of chemical elements in the two rocks were roughly the same, but the amount of each element was different, showing that the main mineral composition in the rock sample is meta-aluminate or silicate and may also contain common coal seam symbiotic minerals, such as gypsum, rock salt, and pyrite.[37]

The mineral composition in the rock sample was qualitatively and semi-quantitatively analyzed by XRD. The results are shown in Figure 4a. The main minerals in the rock samples include quartz; feldspar minerals (albite and potassium feldspar); clay minerals (kaolinite, illite, and chlorite); and a certain amount of calcite, rutile, dolomite, and pyrite. The order of percentage of mineral components in fine sandstone was feldspar minerals (36.0%) > quartz (32.8%) > clay minerals (30.4%). In mudstone, the order was quartz (43.7%) > clay minerals (33.5%) > feldspar minerals (22.8%). Therefore, feldspar

Table 2. Surface Structure and Pore Distribution of Rock Samples

sample	specific surface area (m²/g)				total pore volume (cm³/g)			average pore diameter (nm)			
	BET	Langmuir	BJH adsorption	BJH desorption	single point	BJH adsorption	BJH desorption	BET adsorption	BET desorption	BJH adsorption	BJH desorption
fine sandstone	5.75	7.19	5.51	6.26	0.022	0.022	0.022	15.22	9.04	15.64	13.99
mudstone	8.30	9.73	7.73	8.86	0.027	0.027	0.027	13.07	8.61	13.73	12.17

Table 3. Physiochemical Characteristics of Water Samples[a]

sample	pH	SS (mg/L)	TDS (mg/L)	major ions concentration (mg/L)						
				Na^+	K^+	Ca^{2+}	Mg^{2+}	Cl^-	SO_4^{2-}	HCO_3^-
S1	7.36	2175	1166	338.53	5.81	64.19	15.35	248.67	347.94	292.76
S2	7.5	—	998	359.38	8.34	42.79	1.26	208.17	315.88	252.43
S3	7.48	649	1091	305.70	9.80	66.62	9.35	235.18	339.51	212.65
S4	7.47	—	995	326.72	6.42	45.37	3.72	213.39	300.78	197.48
S5	8.16	—	858	183.05	3.68	82.36	20.54	217.23	258.32	186.24

sample	turbidity NTU	EC (μs/cm)	COD	heavy metal ions concentration (mg/L)						
				Fe	Mn	Cr	Cd	Pb	Cu	Zn
S1	513.40	1960	60.85	0.392	0.0426	0.0142	0.00022	0.0075	0.0027	0.1170
S2	9.32	1522	30.27	0.156	0.0296	0.0091	0.00023	0.0058	0.0043	0.0982
S3	191.30	1955	56.34	0.116	0.0331	0.0090	0.00019	0.0054	0.0038	0.0941
S4	8.12	1530	28.67	0.129	0.0284	0.0087	0.00019	0.0052	0.0030	0.0963
S5	2.93	1267	25.32	0.724	0.0572	0.0117	0.00023	0.0087	0.0078	0.1260

[a]"—" means no detection.

minerals in fine sandstone are higher than in mudstone, whereas clay minerals are lower in sandstone than in mudstone. Furthermore, calcite and pyrite in fine sandstone are slightly higher than those in mudstone. Results from the XRF and XRD analyses, showed the following: K elements were mainly from orthoclase, illite, and mica minerals. Ca elements were mainly from calcite, dolomite, and other impurity minerals. Na elements were mainly from albite and some from mica minerals. Mg elements in the rock samples were mainly from chlorite and some from dolomite or other minerals.[38,39]

The rock samples (fine sandstone and mudstone) were observed by a scanning electron microscopy (SEM). Figure 4b,c show that after crushing, thin plates and strips with irregular sizes and shapes and some irregular microcracks were found on the surface of the minerals. Some studies have shown that the atoms on these edges and micro-cracks may undergo reconstruction and relaxation, making the mineral surface active and leading to certain mineral surface adsorption to some ions in mine water.[40]

The specific surface area of rock minerals can characterize the adsorption properties of substances, and the specific surface area and pore structure of rock samples are listed in Table 2. The specific surface area of fine sandstone was 5.51–7.19 m²/g; that of mudstone was 7.73–9.73 m²/g. The mean of the total pore volume of fine sandstone was 0.027 cm³/g, and that of mudstone was 0.022 cm³/g. The specific surface area and total pore volume of fine sandstone minerals were lower than those of mudstone. The higher specific surface area and total pore volume are more conducive to the adsorption and removal of ions or pollutants in mine water.[41] The measured pore size of fine sandstone was 9.04–15.64 nm, and the mudstone was 8.61–13.73 nm. The pore size of mudstone was less than that of fine sandstone, indicating that the pore distribution in mudstone was denser. Consistent with the specific surface area analysis results, the adsorption capacity of minerals for pollutants in mine water is mudstone > fine sandstone.

In conclusion, compared with mudstone, fine sandstone contains more feldspar minerals, chlorite, muscovite, and calcite, and the dissolution of these minerals will affect the concentration of major ions, such as Na^+, K^+, Ca^{2+}, and Mg^{2+}, in water. The mudstone has denser pores and a larger specific surface area than fine sandstone, so the ion adsorption capacity is stronger.

3.2. Chemical Property Analysis of Water Samples. Fissure water and mine water are the main incoming sources of water in the underground reservoir. Learn the difference in the quality between the two incoming waters from the main physical and chemical composition of the water sample to understand the impact of water quality on the change of ions. The physicochemical characteristics of the collected water samples are summarized in Table 3. The water samples from the underground reservoir in this area were slightly alkaline, and the pH was 7.36–8.16. The average value of influent of SS concentration was 1412 mg/L, and the average turbidity of effluent was 8.72 NTU. The mean value of inlet COD was 58.60, and the mean value of the effluent was 29.47. EC and TDS can be used to characterize the content of dissolved substances. The average values of EC and TDS of the inlet were 1957.5 μs/cm and 1128.5 mg/L, respectively, and those of effluent were 1526 μs/cm and 996.5 mg/L, respectively. Therefore, the pollutant concentration of SS, COD, and dissolved substances from the reservoir water decreased, and fissure water quality was better.

The ions with higher concentrations in the water sample included Na^+, Ca^{2+}, Cl^-, SO_4^{2-}, and HCO_3^-, whereas those with lower concentrations of K^+ and Mg^{2+}. The average concentration of Na^+, Ca^{2+}, Cl^-, SO_4^{2-}, and HCO_3^- in the influent was 322.16, 65.41, 241.93, 343.73, and 252.71 mg/L, respectively, and that of effluent was 343.05, 88.16, 210.78, 308.33, and 224.96 mg/L, respectively. The relative concentration of Ca^{2+} changes greatly, which was 34.78%, whereas the relative concentration of other ions changes less, ranging from 6.48 to 12.88%.
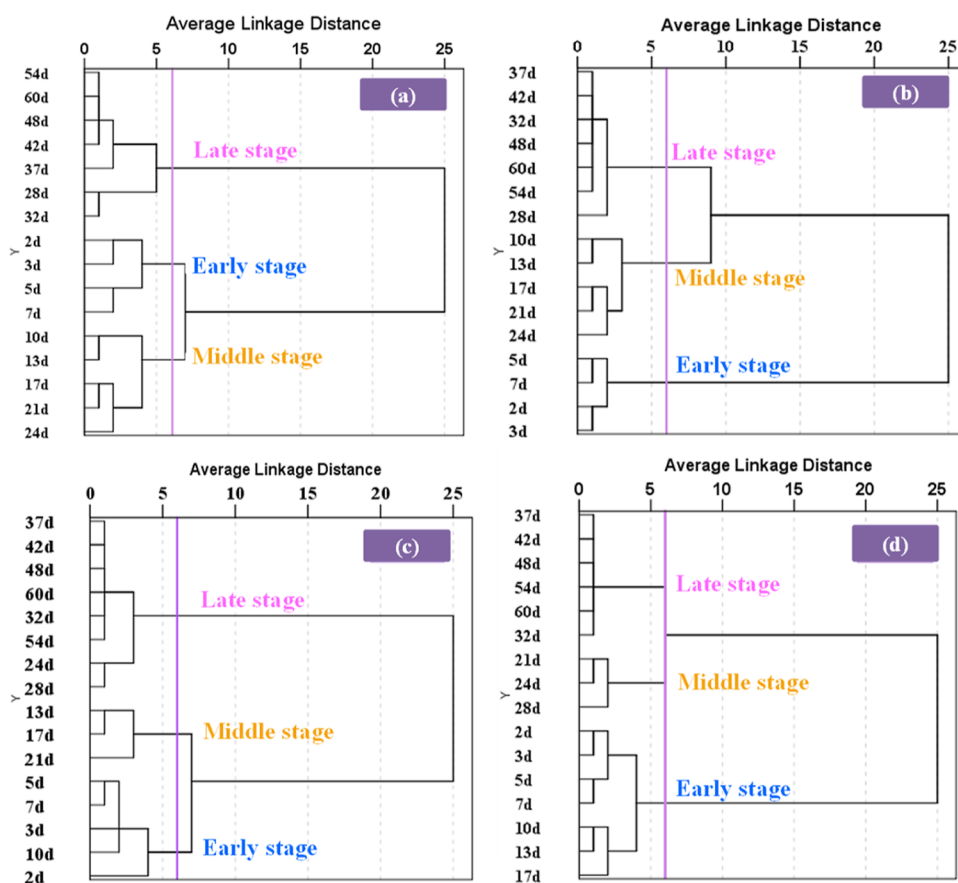
Figure 5. Temporal patterns based on the Q-type HCA method: (a) SM, (b) MM, (c) SMM, and (d) SMF.

From the heavy metal ions, the concentrations of Fe, Mn, and Zn in the collected water samples were relatively high, and the concentrations of Pb, Cd, Cu, and Cr were relatively low.[42] The concentration of heavy metal ions in the effluent of the reservoir decreased to varying degrees, indicating that the caved rock in the coal mine groundwater reservoir had a certain adsorption and removal capacity for heavy metal ions in the mine water.

To sum up, there is a big difference in the concentration of major ions between mine drainage and fissure water. Compared with mine drainage, fissure water has a lower concentration of ions. In the actual operation of an underground reservoir, the mixing effect of mine water intake and overlying fissure water of good quality has a great contribution to the improvement of reservoir effluent quality.

3.3. Determination of the Temporal Patterns of Water−Rock Interaction. Based on the main ion concentration of the water samples in the dynamic simulation experiment, the samples with different reaction times were classified by using the intergroup join (square Euclidean distance) method in the Q-type cluster analysis method, and the system tree diagram was obtained. The appropriate intergroup distance was selected to divide the samples, and different water sample groups divided according to time series could be obtained, as shown in Figure 5. In each group of experiments, the position of the line at a linkage distance of 6 allows a classification of the dendrogram into three clusters, depending on the collection time of water samples. In the SM group, water samples on the 2nd, 3rd, 5th, and 7th days were clustered into the first cluster, water samples on the 10th, 13th, 17th, 21st, and 24th days were clustered into the second cluster,

and water samples on the 28th, 32nd, 37th, 42nd, 48th, 54th, and 60th days were clustered into the third cluster. Considering that the water−rock interaction reaction is continuous, we named the first, second, and third clusters as early, middle, and late stages, respectively, to determine the temporal patterns of the water−rock interaction. In the SM group, the early stage is 0−7 days, the middle stage is 8−24 days, and the late stage is 25−60 days. For the MM experimental group, the early, middle, and late stages are the same as the SM group. It showed that rock properties had no noticeable effect on the determination of the temporal patterns of the water−rock interaction. In the SMM group, the early, middle, and late stages of water−rock interaction were concentrated in 0−10, 11−21, and 22−60 days, respectively, whereas those of the SMF group were concentrated in 0−17, 18−28, and 29−60 days, respectively. Therefore, water quality had a greater impact on the determination of the temporal patterns, different from rock properties.

Based on the temporal patterns, we further observed the time variation of the main cations (Na^+, K^+, Ca^{2+}, and Mg^{2+}) and anions (Cl^-, SO_4^{2-}, and HCO_3^-) in the four experimental groups, as shown in Figure 6. The change in main cations with time in the four experimental groups was similar; that is, in the early and middle stages, the concentration of Na^+ and K^+ increased first and then decreased, and the changing trend of Ca^{2+} and Mg^{2+} showed the opposite. In the late stage, the change of the main cation concentration becomes smaller. With the extension of time, the ion concentration hardly changes anymore, and the system is in a dynamic equilibrium state. However, due to the influence of water quality and rock
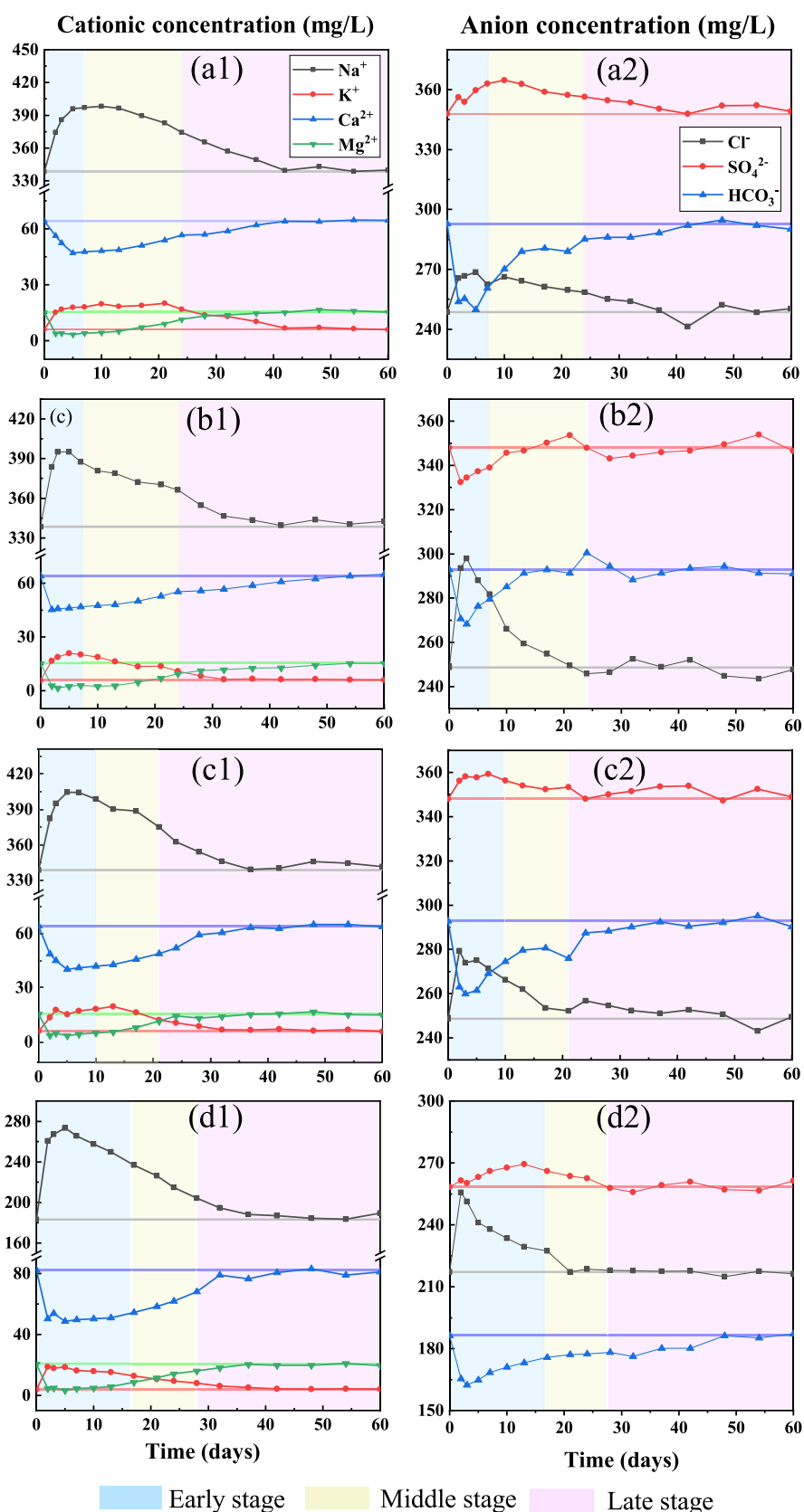
Figure 6. Variation of main ions with time: (a−d) represent SM, MM, SMM, and SMF experimental groups, respectively; 1 and 2 represent cations and anions, respectively.

properties, the time of the inflection point of cation change trends was different for the SM, MM, and SMM groups. The inflection point was mainly concentrated in 3−7 days, similar to

the time point of the early stage of these experimental groups being divided. The variation trend of anion concentration in different groups was dissimilar. In general, in the early and
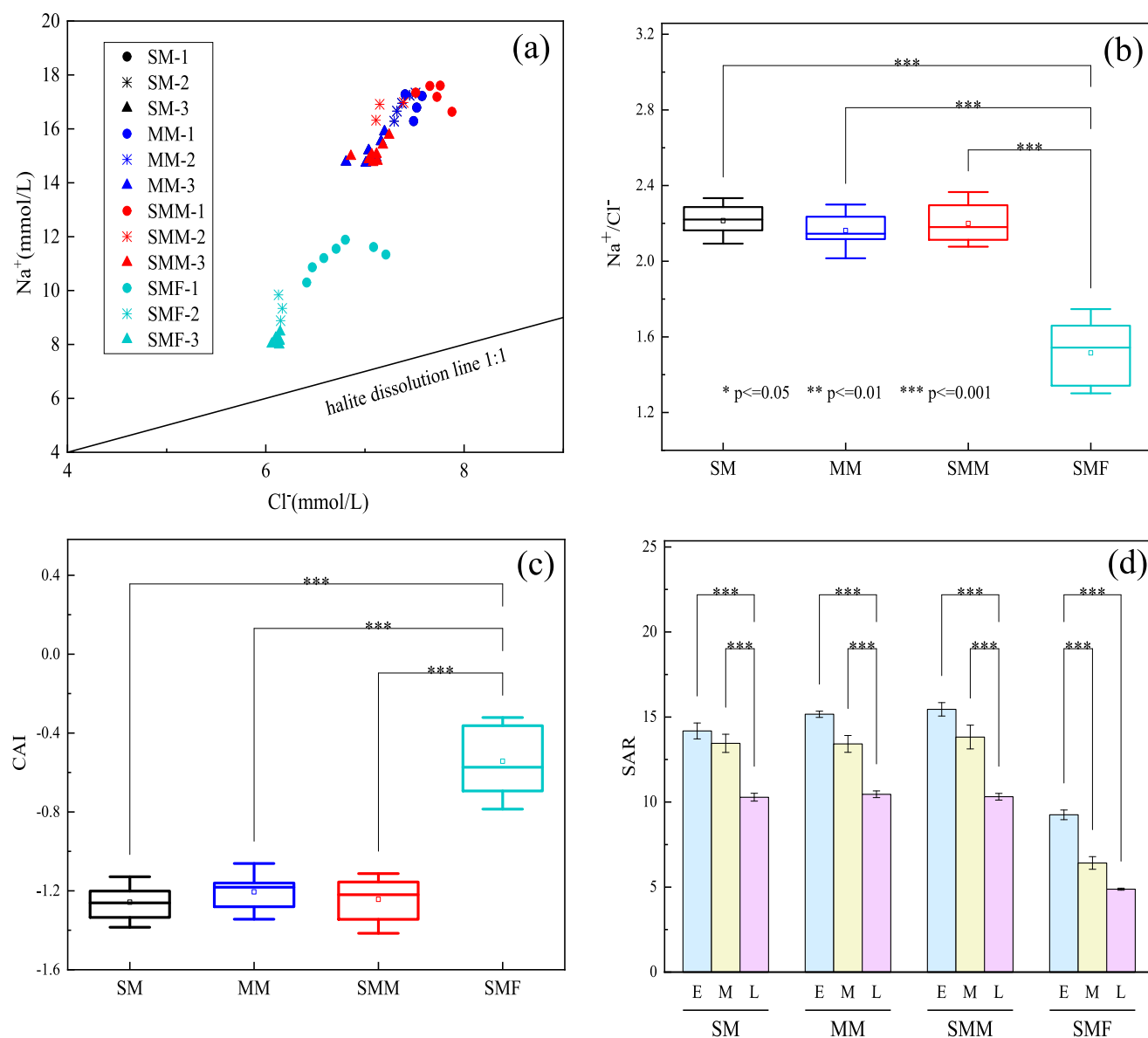
Figure 7. Source analysis of Na+: (a) Na+/Cl−; (b) group differences of Na+/Cl−; (c) group differences of CAI; and (d) group differences of SAR.

middle stages, Cl^- showed a trend of increasing first and then decreasing, while HCO_3^- and Cl^- had the opposite, and in the late stage, the main anion concentration gradually reached the equilibrium state. In SM, SMM, and SMF groups, SO_4^{2-} showed a trend of rising in the early stage and then slowly fluctuating to equilibrium, whereas SO_4^{2-} in the MM group showed a decreasing trend in the early stage. Two different intersection points were found between the change curves of Cl^- and HCO_3^- in the three groups of SM, MM, and SMM. The second intersection point was exactly consistent with the division of the previous stage in the cluster analysis results. The reliability of the Q-type HCA applied to determine the temporal patterns in the water−rock interaction process was confirmed further. The concentration of Cl^- in the SMF group was always higher than that of HCO_3^-. The reason is that the ion concentration in fissure water was low, and the relative abundance was different from that of mine water, which affects the changing trend of ions.[43]

4. DISCUSSION

4.1. Analysis of the Main Ion Sources in Each Stage of Water−Rock Interaction. The ion ratio method was used to analyze the source of the main ions to explore the differences in the types and strengths of the water−rock reaction in each stage. The ion ratio method usually indicates the ion source and the water−rock interaction, providing valuable information on geochemical processes.[44] By the Tukey test, $p < 0.05$ indicates a significant difference between the groups. Two interesting things can be found in Figures 7 and 8: (1) among the various ion ratios, the ions ratios range of the water samples in the SMF group was always significantly different from the other three groups, indicating that water quality differences could affect the intensity of the water−rock reaction. (2) The ion ratio changes regularly with time, and the trend of the change was similar in different groups, which further proved the temporal patterns in the water−rock interaction.

4.1.1. Source Analysis of Na+ in Each Stage of Water−Rock Interaction. In the process of the water−rock interaction, the increase or decrease in the concentration of Na+ was affected by
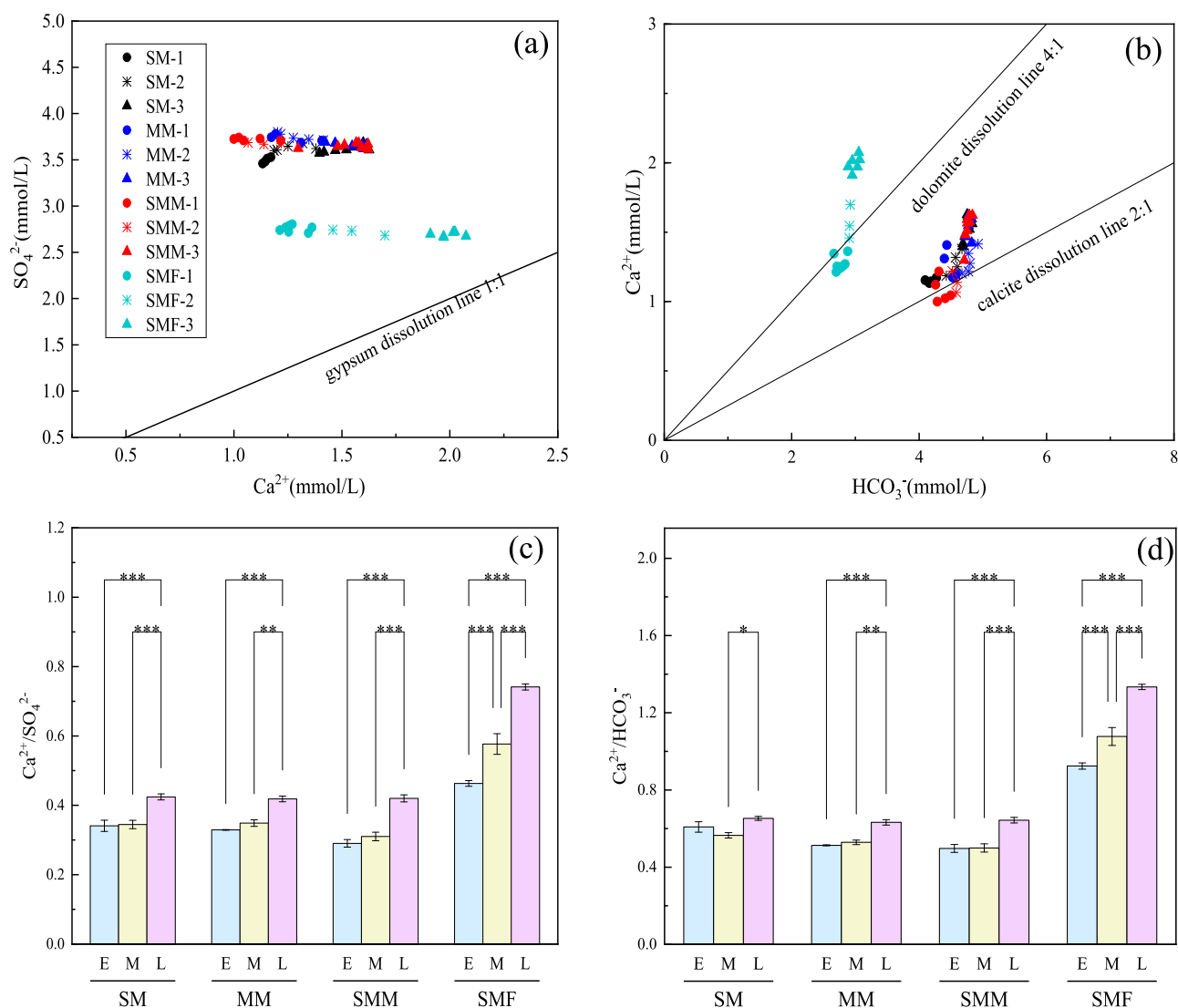
Figure 8. Source analysis of Ca^{2+}, SO_4^{2-}, and HCO_3^-: (a) SO_4^{2-}/Ca^{2+}; (b) Ca^{2+}/HCO_3^-; (c) group differences of Ca^{2+}/SO_4^{2-}; and (d) group differences of Ca^{2+}/HCO_3^-.

many effects, among which mineral dissolution and cation exchange are usually the most obvious.[18,20] Na^+/Cl^- can reflect the deficiency or excess level of Na^+ relative to Cl^-, if Na^+ and Cl^- only come from the dissolution of halite; then according to the chemical composition of halite, the molar concentration ratio of Na^+/Cl^- should be a fixed value of 1. Figure 7a shows that the concentration of Na^+ changes regularly with the increase of Cl^-, and the Na^+/Cl^- of all water samples is less than 1. Na^+ was relatively in excess compared to Cl^-, and the source of Na^+ involved other sources besides halite dissolution. According to the mineral composition analysis, the dissolution of sodium-containing silicate minerals, such as albite, alurgite, and muscovite occurred in fine sandstone and mudstone. Figure 7b shows that the range of Na^+/Cl^- in the SMF group was different from the other three groups. Combined with the analysis of the chemical properties of the water samples, the level of Na^+ in fissure water was lower than that of mine water, whereas the level of Cl^- was higher than that of mine water. As a result, the value of Na^+/Cl^- in the SMF group was significantly lower than that of the other groups. This indicates that the concentration of Na^+ and Cl^- in water affects the dissolution intensity of halite. The study of Yin[45] and Jia[46] also concluded

that the ion concentration in water had a great influence on the dissolution amount and rate of soluble salt minerals.

CAI $(Cl-(Na + K)/Cl)$ is often used to judge whether a cation exchange reaction occurs in the water−rock interaction.[47] As shown in Figure 7c, the values of CAI for the four groups were negative, showing cation exchange in the process.[48] Consistent with the significant difference between groups of Na^+/Cl^-, the CAI value of the SMF group was significantly different from other groups, which further indicated that the relative abundance of Na^+ and Cl^- in water would significantly affect the intensity of the cation exchange reaction during the water−rock interaction. Next, the sodium adsorption ratio (SAR) can be used to identify the strength of cation exchange in the water−rock interaction.[49] Figure 7d shows that the SAR value of the SMF group was lower than that of the other groups, indicating that the cation exchange in the SMF group was relatively weak in the process of the water−rock interaction. From the time stage, the order of SAR values in the four groups was early-stage > middle-stage > late-stage, showing that the cation exchange effect decreased gradually with the extension of the reaction time. Significant difference analysis showed that in SM, MM, and SMM groups, the cation exchange reaction was more intense in

the early and middle stages, whereas the SMF group was only more intense in the early stage. In the SM, MM, and SMM groups, extremely significant differences were observed between the late stage and the other two stages, whereas, in the SMF group, extremely significant differences were observed in all three-time stages.

4.1.2. Source Analysis of Ca^{2+}, SO_4^{2-}, and HCO_3^- in Each Stage of Water−Rock Interaction. Ca^{2+}, SO_4^{2-}, and HCO_3^- were derived from the dissolution of carbonate minerals (such as dolomite and calcite) and evaporated minerals (such as gypsum and anhydrite).[50−52] If Ca^{2+} and SO_4^{2-} only come from gypsum dissolution, the moral concentration ratio of Ca^{2+}/SO_4^{2-} should be a fixed value of 1. If Ca^{2+} and HCO_3^- only come from calcite dissolution, the molar concentration ratio of Ca^{2+}/HCO_3^- should be between 1:1 and 1:2. As shown in Figure 8a,b, the concentration of Ca^{2+} changes regularly with the increase of SO_4^{2-} and HCO_3^-, and Ca^{2+}/SO_4^{2-} and Ca^{2+}/HCO_3^- in all water samples are less than 1. Therefore, the lack of Ca^{2+} relative to SO_4^{2-} and HCO_3^- is mainly related to the relative abundance of Ca^{2+}, SO_4^{2-}, and HCO_3^- in raw water. Furthermore, the cation exchange reaction further leads to a shortage of Ca^{2+}. Combined with the analysis of rock mineral composition, the source of Ca^{2+} may come from the dissolution of dolomite in addition to the dissolution of gypsum and calcite minerals. In addition to gypsum dissolution, the source of SO_4^{2-} may be a small amount from the oxidative hydrolysis of pyrite, and HCO_3^- mainly comes from the dissolution of calcite, dolomite, and other minerals.[53,54]

The levels of Ca^{2+}/SO_4^{2-} and Ca^{2+}/HCO_3^- at different time stages are shown in Figure 8c,d. Combined with the change of main ions with time, Ca^{2+} showed a decreasing trend in the early stage, an increasing trend in the middle stage, and stability in the late stage. The analysis in the previous section shows that the cation exchange reaction is strong in the early stage of water−rock interaction, and the result will lead to an increase in the concentration of Na^+ and a decrease in the concentration of Ca^{2+}. Therefore, in the middle stage, the water−rock reaction of supplying Ca^{2+} concentration is the main reaction, which may include the dissolution of calcium-containing minerals, such as calcite, dolomite, and gypsum. Unlike the MM group, in the SM group, the Ca^{2+}/SO_4^{2-} in the middle stage was slightly lower than in the early stage. Combined with mineral composition analysis, calcite and dolomite were found to be contained in fine sandstone rather than mudstone and were dissolved, promoting the precipitation of HCO_3^- and reducing the ratio of Ca^{2+}/HCO_3^-. Therefore, the dissolution reaction of the carbonate minerals, such as calcite and dolomite, is more intense in the middle stage of the water−rock interaction. This is basically consistent with the previous use of soil column experiments to study the dissolution behavior of carbonate minerals in the water−rock interaction during the infiltration of surface water polluted by mine water, that is, it increases first and then decreases until it is stable.[55]

4.2. Type and Intensity of Main Water−Rock Interaction at Each Stage. According to Sections 3.3 and 3.4, given the influence of water quality, the temporal pattern and the change rule of ion concentration were quite different from the other groups. PCA was conducted to decompose the variables of ions, such as Ca^{2+}, Mg^{2+}, Na^+, K^+, HCO_3^-, Cl^-, and SO_4^{2-}, in the SMF water samples. The results showed that all indexes were reduced to 1 dimension; thus, it was not suitable for PCA. Similarly, 48 samples in the SM, MM, and SMM groups were analyzed using PCA to decompose variables of ions, and the

results are shown in Tables 4 and 5. As shown in Table 4, the Kaiser−Meyer−Olkin was 0.759, and Bartlett's test of sphericity

Table 4. Correlation Matrix for Factor Analysis

component	initial eigenvalues			statistical test
	total	variance (%)	cumulative (%)	
1	5.019	71.704	71.704	
2	1.184	16.911	88.615	
3	0.441	6.297	94.912	KMO = 0.759
4	0.152	2.179	97.090	Sig = 0.000
5	0.111	1.587	98.677	
6	0.076	1.082	99.760	
7	0.017	0.240	100.000	

Table 5. Component Matrix after Rotation

index	factor	
	1	2
Na^+	0.959	0.209
K^+	0.925	0.135
Ca^{2+}	−0.933	−0.056
Mg^{2+}	−0.954	0.020
Cl^-	0.884	−0.299
SO_4^{2-}	0.067	0.990
HCO_3^-	0.797	−0.301

declined, indicating that the data were correlated, and the factor analysis was effective. With two principal components, the cumulative contribution rate was greater than 80%, and the information extraction rate of each variable was greater than 0.70.[56,57] The two principal components can better reflect most of the information of the original variables, and the effect of PCA is good. As shown in Table 5, ions of Na^+, K^+, Ca^{2+}, Mg^{2+}, Cl^-, and HCO_3^- possessed high loading values in the PC_1 direction, whereas the ion of SO_4^{2-} had a high loading value in the PC_2 direction. According to the above analysis, PC_1 can represent cation exchange and the dissolution of minerals (such as halite, calcite, and dolomite), and PC_2 can represent the oxidative hydrolysis of pyrite and the adsorption of minerals.[58,59] The oxidative hydrolysis of pyrite leads to an increase in the concentration of SO_4^{2-}, whereas the adsorption of minerals leads to a decrease in the concentration of SO_4^{2-}. The two effects have opposite effects and need to be analyzed with the actual situation.

The factor score diagram of each water sample was drawn, taking the common factors PC_1 and PC_2 as the coordinate axes, as shown in Figure 9. The load distributions on PC_1 and PC_2 of the water samples in the early, middle, and late stages were different. Most of the water samples in the early and middle stages were distributed in the positive direction of PC_1, indicating that the main water−rock reaction in the early and middle stages included the cation exchange and the dissolution of minerals, such as halite, calcite, dolomite, and gypsum. Based on analysis of the ion source, the early stage of water−rock interaction could be dominated by cation exchange, supplemented by mineral dissolution. In contrast, the middle stage was dominated by mineral dissolution, supplemented by cation exchange. The water samples from the late stage were distributed in the negative direction of PC_1, showing that the cation exchange is weak in the late stage and that the dissolution of minerals has reached equilibrium. The early water samples of SM and SMM were distributed in the positive direction of PC_2,
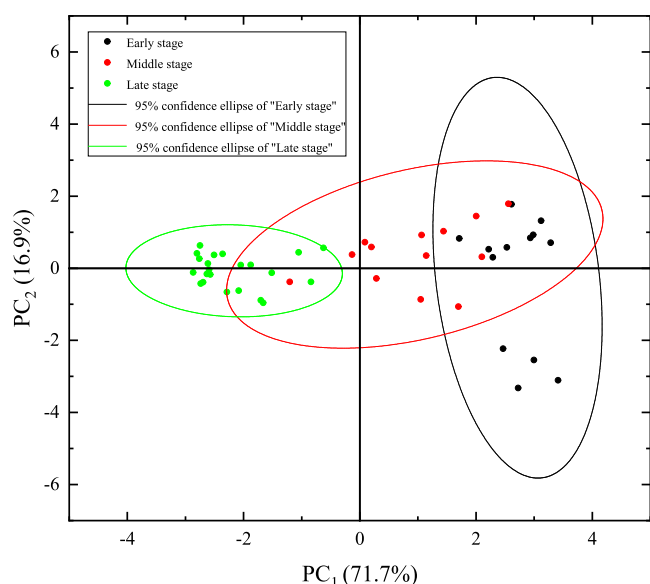
Figure 9. PCA plot of the hydro-chemical of the SM, MM, and SMM experimental samples.

whereas those of MM were distributed in the negative direction of PC_2. According to the mineral composition and ion change, the mudstone contains more clay minerals than the fine sandstone and almost no pyrite, resulting in a lower SO_4^{2-} content in the MM formation than in the SM and SMM formations in the early stage. Therefore, the positive direction of PC_2 can explain the strength of oxidative hydrolysis of pyrite,

whereas the negative direction can explain the strength of the adsorption of minerals. The water samples in the middle and late stages were relatively evenly distributed in the positive and negative directions on PC_2, and the load was small, indicating that the oxidation hydrolysis reaction of pyrite and the adsorption of clay minerals in the middle and later stages of the water−rock interaction was weak. The water samples in the middle and late stages were evenly distributed in the positive and negative directions on PC_2, and the load was small. The oxidation hydrolysis reaction of pyrite and mineral adsorption was weak in the middle and late stages of the water−rock interaction. The influence of different components and contents of soluble minerals and clay-like minerals in the rocks on the type and intensity of water−rock interaction in each stage is different, which is basically consistent with the results of previous studies on the mechanism of the influence of rock mineral characteristics on the water−rock interaction.[60]

In summary, the temporal pattern of water−rock interaction can be determined by the Q-type HCA method. Combined with the ion ratio method and PCA method, the main types and intensity of water−rock interaction in each stage can be further analyzed. The above research methods provide new ideas for revealing the mechanism of the water−rock interaction, such as the application in the geochemical aspects of natural gas hydrate exploitation and exploration.[61,62] The research shows that, in general, the water−rock interaction process between the collapsed rock (fine sandstone and mudstone) and the main water (mine water and fissure water) in the underground reservoir can be divided into three time stages: early, middle, and late. The specific stage division and mechanism of action are shown in Figure 10. The early stage of water−rock interaction is
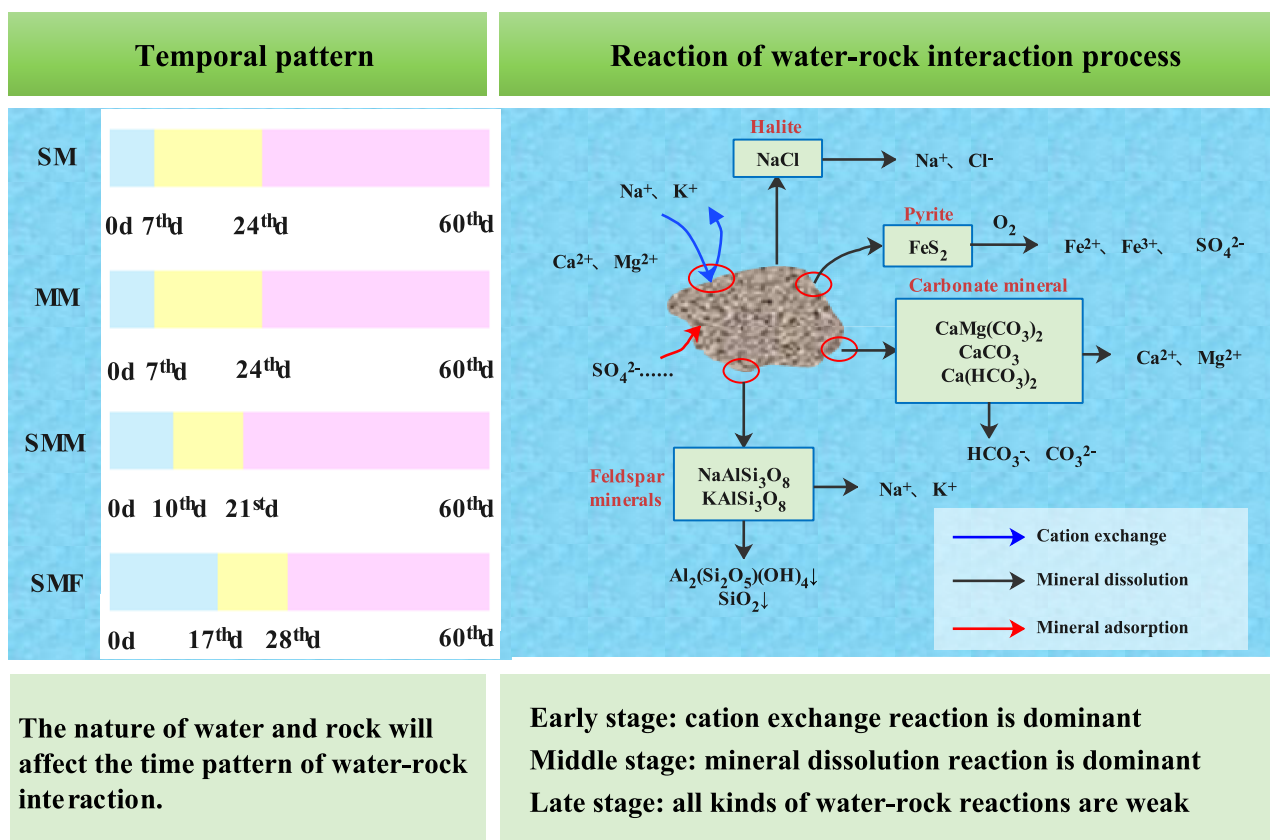

Figure 10. Temporal pattern and mechanism of the water−rock interaction.

dominated by the cation exchange reaction, in addition to the dissolution of soluble minerals, such as halite and calcite, and the adsorption of clay minerals. The middle stage of the water−rock interaction is dominated by mineral dissolution, supplemented by the cation exchange reaction and mineral adsorption. In the late stage of the water−rock interaction, the water−rock reaction is weak and in a dynamic equilibrium state, which is basically consistent with previous studies.[63] The nature of water and rock will affect the type and intensity of the water−rock interaction in each stage, and the nature of water has a greater impact. The research results are of great significance for the prediction of groundwater reservoir effluent ions. According to the conclusion of this study, it can be seen that in this system, the cation exchange reaction is the dominant roles in the early stages, so the concentration of Ca^{2+} decreased during this period by about 1/2 the amount that of the concentration of Na^+ increased. It is worth noting that during the actual operation of the underground reservoir in the coal mine; the water−rock interaction process is often affected by the mixing action of the newly incoming water and the overlying fissure water, which causes relatively large changes in the ion concentration. The ion concentration in the later stage can be estimated based on the initial ion concentration and flow of the two incoming waters.

5. CONCLUSIONS

In the actual operation of underground reservoirs in coal mines, the concentration level of ions in the effluent is closely related to the length of residence time. Based on field monitoring, this paper designed a dynamic simulation experiment of the water−rock interaction aimed at the comparison of water quality and rock properties and explored the temporal patterns of the water−rock interaction, as well as the source of ions in each stage and the type and intensity of the water−rock interaction. This study shows that the water−rock interaction can be divided into early, middle, and late stages and that water quality has more influence on the temporal patterns than rock properties. The types and intensities of the water−rock interaction were different at different time stages. Generally speaking, the early stage was dominated by cation exchange, the middle stage was dominated by mineral dissolution, and the late stage was relatively weak with little relative change in ion concentration. In practice, the mixing between the overlying fissure water of good quality and the mine water will further dilute the ion concentration in the water and improve the effluent quality of the reservoir. The research conclusion has a certain practical value for guiding the prediction of effluent ion concentration in underground reservoirs and the selection and optimization of subsequent water quality assurance measures. However, this paper only considers the change rule of main ions with time and does not consider the change rule of concentration of suspended solids, COD, heavy metals, and other pollutants with time and their coupling effect. It is suggested that further research be carried out later.

■ AUTHOR INFORMATION

Corresponding Author

Kai Zhang − *School of Chemistry and Environment, China University of Mining and Technology (Beijing), Beijing 100083, China;* ● orcid.org/0000-0001-7735-7663; Phone: 010-62339810; Email: zhangkai@cumtb.edu.cn

Authors

Shuyu Liu − *School of Chemistry and Environment, China University of Mining and Technology (Beijing), Beijing 100083, China*

Ju Gao − *School of Chemistry and Environment, China University of Mining and Technology (Beijing), Beijing 100083, China*

Yingming Yang − *State Key Laboratory of Water Resource Protection and Utilization in Coal Mining, Beijing 102211, China; National Institute of Clean-and-Low Carbon Energy, Beijing 102211, China*

Lu Bai − *State Key Laboratory of Water Resource Protection and Utilization in Coal Mining, Beijing 102211, China; National Institute of Clean-and-Low Carbon Energy, Beijing 102211, China*

Jiayu Yan − *School of Chemistry and Environment, China University of Mining and Technology (Beijing), Beijing 100083, China*

Complete contact information is available at:
https://pubs.acs.org/10.1021/acsomega.2c08145

■ REFERENCES

(1) Cheng, A.; Ning, S.; Yuan, T. A study on coal resource comprehensive regionalization in china. *Coal Geology of China* **2011**, *23*, 5−8.

(2) Cao, H.-D. Study on water resources development and utilization in water shortage large coal mining area. *Coal Sci. Technol.* **2011**, *39*, 110−113.

(3) Lu, X. Present situation and suggestion for clean coal development and utilization in china. *Coal Engineering* **2015**, *48* (3), 8−10.

(4) Wang, L.; Wei, S.-P.; Wang, Q.-J. Effect of coal exploition on groundwater and vegetation in the yushenfu coal mine. *J. China Coal Soc.* **2008**, *33*, 1408−1414.

(5) Gu, D. Water resource and surface ecology protection technology of modern coal mining in china's energy golden triangle. *Strategic Study of CAE* **2013**, *15*, 102−107.

(6) Wu, Q. Progress,problems and prospects of prevention and control technology of mine water and reutilization in china. *J. China Coal Soc.* **2014**, *39*, 795−805.

(7) Limin, F.; Xiongde, M.; Ruijun, J. Progress in engineering practice of water-preserved coal mining in western eco-environment frangible area. *J. China Coal Soc.* **2015**, *40*, 1711−1717.

(8) Gu, D. Z. Water resource protection and utilization engineering technology of coal mining in "energy golden triangle" region. *Coal Engineering* **2014**, *46*, 34−37.

(9) Gu, D.-Z. Theory framework and technological system of coal mine underground reservoir. *J. China Coal Soc.* **2015**, *40*, 239−246.

(10) Gu, D.; Zhang, Y.; Cao, Z. Technical progress of water resource protection and utilization by coal mining in china. *Coal Sci. Technol.* **2016**, *44*, 1−7.

(11) Chen, S.; Huang, Q.; Xue, G.; Li, R. Technology of underground reservoir construction and water resource utilization in daliuta coal mine. *Coal Sci. Technol.* **2016**, *44* (8), 21−28.

(12) Shi, X. Research progress and prospect of underground mines in coal mines. *Coal Sci. Technol.* **2022**, *50* (10), 216−225.

(13) Chen, S. *Research on the Key Technology of Water Resources Recycling Utilization in the Underground Goaf Reservoir in Shendong Mining Area*; Xi'an University of Science and Technology, 2016.

(14) Han, J. Analysis of the source of dom in underground reservoir of coal mine. *J. Min. Sci. Technol.* **2020**, *5*, 575−583.

(15) Zhang, K.; Gao, J.; Men, D.; Zhao, X.; Wu, S. Insight into the heavy metal binding properties of dissolved organic matter in mine water affected by water−rock interaction of coal seam goaf. *Chemosphere* **2021**, *265*, 129134.

(16) Han, J. M.; Gao, J.; Du, K.; Chen, M.; Jiang, B.; Zhang, K. Analysis of hydrochemical characteristics and formation mechanism in coal mine underground reservoir. *Coal Sci. Technol.* **2020**, *48*, 223−231.

(17) Binbin, J.; Shuyu, L.; Jie, R.; Ranfeng, Z.; Mengyuan, C.; Yan, Y.; Kai, Z. Purification effect of coal mine groundwater reservoir on mine water containing organic compounds and heavy metals in diffencent occurrence forms. *Coal Engineering* **2020**, *52*, 122−127.

(18) Fang, M.; Li, X.; Zhang, G.; Liu, Q.; Tuo, K.; Liu, S. Discussion on water−rock interaction mechanism in underground reservoir of daliuta coal mine. *Coal Sci. Technol.* **2022**, *50* (11), 236−242.

(19) Zhang, K.; Li, H.; Han, J.; Jiang, B.; Gao, J. Understanding of mineral change mechanisms in coal mine groundwater reservoir and their influences on effluent water quality: a experimental study. *Int. J. Coal Sci. Technol.* **2020**, *8*, 154−167.

(20) Zhang, K.; Gao, J.; Jiang, B.; Han, J.; Chen, M. Experimental study on the mechanism of water−rock interaction in the coal mine underground reservoir. *J. China Coal Soc.* **2019**, *44*, 3760−3772.

(21) Li, W. *Dynamic Adsorption Characteristics of Crushed Gangue to Ions in Coal Mine Underground Reservoirs under Leaching Condition*; China University of Mining and Technology, 2021.

(22) Cao, Z. G.; He, R. M.; Wang, X. F. Coal mining affected to underground water and underground water storage and utilization technology. *Coal Sci. Technol.* **2014**, *42*, 113−116.

(23) Guo, Q. Technical progress of underground mine water treatment and zero discharge of waste water. *Clean Coal Technol.* **2018**, *24*, 33−37.

(24) Pan, Z. *Study of Water−Rock Interaction in Chencun Dam-Site*; HoHai University, 2007.

(25) Barzegar, R.; Asghari Moghaddam, A.; Nazemi, A. H.; Adamowski, J. Evidence for the occurrence of hydrogeochemical processes in the groundwater of khoy plain, northwestern iran, using ionic ratios and geochemical modeling. *Environ. Earth Sci.* **2018**, *77*, 597−617.

(26) Demlie, M.; Wohnlich, S.; Wisotzky, F.; Gizaw, B. Groundwater recharge, flow and hydrogeochemical evolution in a complex volcanic aquifer system, central ethiopia. *Hydrogeol. J.* **2007**, *15*, 1169−1181.

(27) Li, P.; Qian, H.; Wu, J.; Zhang, Y.; Zhang, H. Major ion chemistry of shallow groundwater in the dongsheng coalfield, ordos basin, china. *Mine Water Environ.* **2013**, *32*, 195−206.

(28) Karroum, M.; Elgettafi, M.; Elmandour, A.; Wilske, C.; Himi, M.; Casas, A. Geochemical processes controlling groundwater quality under semiarid environment: a case study in central morocco. *Sci. Total Environ.* **2017**, *609*, 1140−1151.

(29) Singh, C. K.; Kumar, A.; Shashtri, S.; Kumar, A.; Kumar, P.; Mallick, J. Multivariate statistical analysis and geochemical modeling for geochemical assessment of groundwater of delhi, india. *J. Geochem. Explor.* **2017**, *175*, 59−71.

(30) Hao, C. m.; Huang, Y.; Ma, D. j.; Fan, X. Hydro-geochemistry evolution in ordovician limestone water induced by mountainous coal mining: a case study from north china. *J. Mt. Sci.* **2020**, *17*, 614−623.

(31) Zhu, B.; Wang, X.; Rioual, P. Multivariate indications between environment and ground water recharge in a sedimentary drainage basin in northwestern china. *J. Hydrol.* **2017**, *549*, 92−113.

(32) Liu, F.; Zhao, Z.; Yang, L.; Ma, Y.; Xu, Y.; Gong, L.; Liu, H. Geochemical characterization of shallow groundwater using multivariate statistical analysis and geochemical modeling in an irrigated region along the upper yellow river, northwestern china. *J. Geochem. Explor.* **2020**, *215*, 106565.

(33) Guler, C.; Thyne, G. D. Hydrologic and geologic factors controlling surface and groundwater chemistry in indian wells-owens valley area, southeastern california, usa. *J. Hydrol.* **2004**, *285*, 177−198.

(34) Ma, Z.; Zhou, M. Application of cluster analysis in correlation study on water quality indexes. *Journal of China Hydrology* **2018**, *38*, 77−80.

(35) Song, H.; Xu, J.; Fang, J.; Cao, Z.; Yang, L.; Li, T. Potential for mine water disposal in coal seam goaf: investigation of storage coefficients in the shendong mining area. *J. Cleaner Prod.* **2020**, *244*, 118646.

(36) Wang, Q.; Li, W.; Li, T.; Li, X.; Liu, S. Goaf water storage and utilization in arid regions of northwest china: a case study of shennan coal mine district. *J. Cleaner Prod.* **2018**, *202*, 33−44.

(37) Jiang, B.; Gao, J.; Du, K.; Deng, X.; Zhang, K. Insight into the water−rock interaction process and purification mechanism of mine water in underground reservoir of daliuta coal mine in china. *Environ. Sci. Pollut. Res.* **2022**, *29*, 28538−28551.

(38) Tao, S.; Bi-wan, X.; Hui-sheng, S. The evolution of coal gangue (cg)−calcium hydroxide (ch)−gypsum−h2o system. *Mater. Struct.* **2007**, *41*, 1307−1314.

(39) Chander, V.; Tewari, D.; Negi, V.; Singh, R.; Upadhyaya, K.; Aleya, L. Structural characterization of himalayan black rock salt by sem, xrd and in-vitro antioxidant activity. *Sci. Total Environ.* **2020**, *748*, 141269.

(40) Pearce, J. K.; Turner, L.; Pandey, D. Experimental and predicted geochemical shale-water reactions; Roseneath and murteree shales of the cooper basin. *Int. J. Coal Geol.* **2018**, *187*, 30−44.

(41) Yao, Q.; Wang, W.; Xia, Z.; Wang, A.; Yu, L. Adsorption characteristics of mn (ii) on sandy mudstone and fine sandtone of coal measures. *J. China Univ. Min. Technol.* **2020**, *49*, 411−418.

(42) Shao, L. N.; He, X. W.; Huang, J. H.; He, Y.; Li, Y. Migration and diffusion of pollutants in the mine water with high turbidity, high concentration of iron and manganese in goaf. *J. China Univ. Min. Technol.* **2009**, *38*, 135−139.

(43) Jia, X. *Research of Groundwater Chemical Characteristics and Pollution in the da bao dang of shenmu*; Xi'an University of Science and Technology, 2014.

(44) Moya, C. E.; Raiber, M.; Taulis, M.; Cox, M. E. Hydrochemical evolution and groundwater flow processes in the galilee and eromanga basins, great artesian basin, australia: a multivariate statistical approach. *Sci. Total Environ.* **2015**, *508*, 411−426.

(45) Yin, Z.; Luo, Q.; Wu, J.; Xu, S.; Wu, J. Identification of the long-term variations of groundwater and their governing factors based on hydrochemical and isotopic data in a river basin. *J. Hydrol.* **2021**, *592*, 125604.

(46) Jia, W. F.; Yang, Y.; Zhao, Y.; Juan, L. I.; Ning-Qing, L.; Bei-Dou, X. I.; Ming-Xiao, L. I.; Yang, J. J.; Guo, Y. F. *Simulation of the Water−Rock Reaction in Chaobai River Ground-Water Storage Area*; South-to-North Water Transfers and Water Science & Technology, 2016.

(47) Gaofeng, Z.; Yonghong, S.; Chunlin, H.; Qi, F.; Zhiguang, L. Hydrogeochemical processes in the groundwater environment of heihe river basin, northwest china. *Environ. Earth Sci.* **2010**, *60*, 139−153.

(48) Li, P.-Y.; Qian, H.; Wu, J.-H.; Ding, J. Geochemical modeling of groundwater in southern plain area of pengyang county, ningxia, china. *Water Sci. Eng.* **2010**, *3*, 282−291.

(49) Che, Q.; Su, X.; Wang, S.; Zheng, S.; Li, Y. Hydrochemical characteristics and evolution of groundwater in the alluvial plain (anqing section) of the lower yangtze river basin: multivariate statistical and inversion model analyses. *Water* **2021**, *13*, 2403.

(50) Liu, F.; Wang, S.; Wang, L.; Shi, L.; Song, X.; Yeh, T. C. J.; Zhen, P. Coupling hydrochemistry and stable isotopes to identify the major

factors affecting groundwater geochemical evolution in the heilongdong spring basin, north china. *J. Geochem. Explor.* **2019**, *205*, 106352.

(51) Zhou, J.-M.; Jiang, Z.-C.; Xu, G.-L.; Qin, X.-Q.; Huang, Q.-B.; Zhang, L.-K. Major ionic characteristics and controlling factors of karst groundwater at xiangshui, chongzuo. *Environ. Sci.* **2019**, *40*, 2143−2151.

(52) Chen, K.; Sun, L.; Xu, J. Statistical analyses of groundwater chemistry in the qingdong coalmine, northern anhui province, china: implications for water−rock interaction and water source identification. *Appl. Water Sci.* **2021**, *11*, 50.

(53) Huang, S.; Huang, S.; Feng, W.; Tong, H.; Liu, L.; Zhang, X. Mass exchanges among feldspar, kaolinite and illite and their influences on secondary porosity formation in clastic diagenesis—a case study on the upper paleozoic, ordos basin and xujiahe formation, western sichuan depression. *Geochimica* **2009**, *38*, 498−506.

(54) Li, Z.; Wang, G.; Wang, X.; Wan, L.; Shi, Z.; Wanke, H.; Uugulu, S.; Uahengo, C. I. Groundwater quality and associated hydrogeochemical processes in northwest namibia. *J. Geochem. Explor.* **2018**, *186*, 202.

(55) Wu, Y. G.; Shen, Z. L.; Zhong, Z. S.; Guang-He, L. I. *Water−Rock Interaction during Irrigation with Polluted Water by Coal Mine Drainage*; Coal Geology & Exploration, 2004.

(56) Ravikumar, P.; Somashekar, R. K. Principal component analysis and hydrochemical facies characterization to evaluate groundwater quality in varahi river basin, karnataka state, india. *Appl. Water Sci.* **2015**, *7*, 745−755.

(57) Yang, F.; Liu, S.; Jia, C.; Gao, M.; Chang, W.; Wang, Y. Hydrochemical characteristics and functions of groundwater in southern laizhou bay based on the multivariate statistical analysis approach. *Estuarine, Coastal Shelf Sci.* **2021**, *250*, 107153.

(58) Sun, J.; Kobayashi, T.; Strosnider, W. H. J.; Wu, P.; Werner, A. D.; Post, V. E. A. Stable sulfur and oxygen isotopes as geochemical tracers of sulfate in karst waters. *J. Hydrol.* **2017**, *551*, 245−252.

(59) Jia, H.; Qian, H.; Zheng, L.; Feng, W.; Wang, H.; Gao, Y. Alterations to groundwater chemistry due to modern water transfer for irrigation over decades. *Sci. Total Environ.* **2020**, *717*, 137170.

(60) Wang, Z.; Hao, R.; Yang, H.; Wang, W.; Yang, S. Research progress on water-rock interaction. *J. Water Resour. Environ. Eng.* **2015**, *26*, 210−216.

(61) Ren, J.; Liu, X.; Niu, M.; Yin, Z. Effect of sodium montmorillonite clay on the kinetics of ch4 hydrate - implication for energy recovery. *Chem. Eng. J.* **2022**, *437*, 135368.

(62) Yin, Z.; Linga, P. Methane hydrates: a future clean energy resource. *Chin. J. Chem. Eng.* **2019**, *27*, 2026−2036.

(63) Zhang, K.; Liu, S. Y.; Cao, Z. G.; Gao, J.; Chen, X. Y.; Yan, J. Y. Study on the time law of water-rock interaction in coal mine groundwater reservoir. *Coal Geol. Explor.* **2023**, 1−10.